pubs.acs.org/Biomac

Article

Effect of Hydrophobic Groups on Antimicrobial and Hemolytic Activity: Developing a Predictive Tool for Ternary Antimicrobial Polymers

Pham Thu Phuong, Susan Oliver, Junchen He, Edgar H. H. Wong, Robert T. Mathers,* and Cyrille Boyer*

Cite This: https://dx.doi.org/10.1021/acs.biomac.0c01320

Read Online

ABSTRACT: Antimicrobial polymers have emerged as a potential solution to the growing problem of antimicrobial resistance. Although several studies have examined the effects of various parameters on the antimicrobial and hemolytic activity of statistical copolymers, there are still numerous parameters to be explored. Therefore, in this study, we developed a library of 36 statistical amphiphilic ternary copolymers prepared via photoinduced electron transfer-reversible addition−fragmentation chain transfer polymerization to systematically evaluate the influence of hydrophobic groups [number of carbons (5, 7, and 9)] and chain type of the hydrophobic monomer (cyclic, aromatic, linear, or branched), monomer ratio, and degree of polymerization (DP_n) on antimicrobial and hemolytic activity. To guide our synthetic strategy, we developed a pre-experimental screening approach using *C* log *P* values of oligomer models, which correspond to the logarithm of the partition coefficient of compounds between *n*-octanol and water. This method enabled correlation of polymer hydrophobicity with antimicrobial and hemolytic activity. In addition, this study revealed that minimizing hydrophobicity and hydrophobic content were key factors in controlling hemolysis, whereas optimizing antimicrobial activity was more complex. High antimicrobial activity required hydrophobicity (i.e., *C* log *P*, hydrophobicity index) that was neither too high nor too low, an appropriate cationic/hydrophobic balance, and structural compatibility between the chosen monomers. Furthermore, these findings could guide the design of future antimicrobial ternary copolymers and suggest that *C* log *P* values between 0 and 2 have the best balance of high antimicrobial activity and low hemolytic activity.

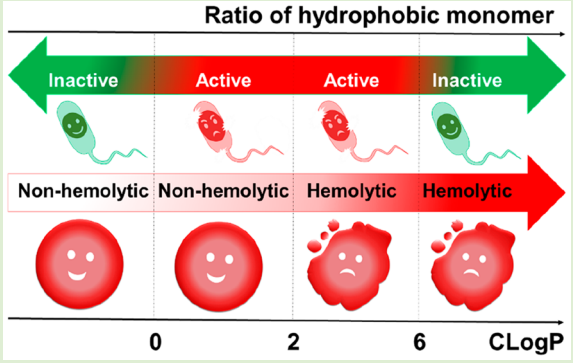

INTRODUCTION

Since the discovery of the first antibiotic, penicillin, in 1928, the mortality from bacterial infections has been significantly reduced. However, antibiotic misuse and overuse in farming and medicine has resulted in the emergence of antibiotic resistance, which is recognized as one of the most pressing health issues worldwide.[1−3] According to the World Health Organization, antimicrobial resistance accounts for an estimated 700,000 deaths each year.[4] More precisely, the "ESKAPE" pathogens, *Enterococcus faecium*, *Staphylococcus aureus*, *Klebsiella pneumoniae*, *Acinetobacter baumannii*, *Pseudomonas aeruginosa*, and *Enterobacter* species, have developed strains that are antibiotic-resistant against a broad range of antibiotics.[5] In addition, despite considerable effort, no new classes of antibiotics have been approved for Gram-negative pathogens in over 50 years.

There is an urgent need, therefore, to develop alternative antimicrobial agents.[6−13] A potential alternative to current antibiotic agents is the use of antimicrobial peptides,[14,15] which are part of the innate immune system of many organisms. These host defence peptides are locally produced by various cells to help protect against continuous exposure to microorganisms. Encouragingly, these peptides have been recognized as promising antimicrobial compounds capable of efficiently combatting antibiotic resistance owing to their mode of action.[6,16−21] These peptides comprise a small number of amino acid residues (usually, between 10 and 50 residues), containing hydrophobic, cationic, and hydrophilic groups. Their amphiphilic nature allows them to interact with bacterial cell membranes, resulting in the disruption of bacterial cells. The presence of cationic charges allows them to interact with negatively charged bacterial cell walls, while the hydrophobic groups facilitate insertion and disruption of the phospholipid membranes. Despite their promise, there are limitations with

Received: September 9, 2020
Revised: October 29, 2020

the use of these natural peptides as they are expensive to develop and produce in large quantities and are also subject to proteolysis, which reduces their long-term stability in biological environments.

Inspired by the structure of these peptides and thanks to advancements in polymer chemistry, particularly controlled/living polymerization, antimicrobial polymers have been proposed as potential alternatives.[6−13,20,22−26] Unlike their peptide counterparts, these antimicrobial polymers can be produced on a large scale and are less susceptible to proteolysis. These advantages have led to a number of statistical amphiphilic antimicrobial polymers being prepared from a variety of monomers, such as (meth)acrylate,[20,27−31] acrylamide,[32,33] 3-aminopropanoic acid,[34,35] norbornene,[36,37] phenyleneethynylene,[38] maleimide,[39] quaternary vinylpyridine,[40] urea,[41] and oxetane.[42] Although these polymers exhibit high antimicrobial activity, they are often not specific to bacterial cells and, therefore, kill mammalian and bacterial cells without discrimination, resulting in high toxicity for the host and reducing their potential applications. To overcome this major limitation, researchers have tried to identify key factors that allow reduction in their toxicity against mammalian cells without affecting their antimicrobial performance.[43,44] For instance, the molecular weight of these polymers influences their biocompatibility. An increase in molecular weight often results in an increase in hemolytic activity but their antimicrobial activity is not significantly impacted. More importantly, the composition of these copolymers, such as their amphiphilic balance,[45,46] has a more significant impact on their biocompatibility and antimicrobial activity.[47−50] To control the amphiphilic balance, these polymers are prepared by copolymerization of hydrophobic and cationic monomers and, in some instances, the inclusion of some hydrophilic monomers. The number and type of cationic groups, as well as the type of hydrophobic monomers, employed for their syntheses exhibit a significant impact on their selectivity toward bacterial cells.[51] As the cationic groups are the ones that facilitate the adsorption of polymers on the anionic bacterial membrane via electrostatic interaction, different cationic groups have been investigated to gain insight into the structural effect of these components on overall bioactivity.[16,18,20] One of the most common choices for antimicrobial cationic monomers is monomers functionalized with an amino group, including primary, secondary, tertiary, and quaternary groups. Judzewitsch[33] and Palermo[31] demonstrated that amphiphilic copolymers containing primary amines display high antimicrobial activity against Gram-negative bacteria, whereas those containing quaternary ammonium groups are more efficient against mycobacteria (*Mycobacterium smegmatis*).[33] Ragogna, Gillies, and co-workers proposed the introduction of phosphonium groups as alternatives to amino groups.[7,8] As the hydrophobic groups disrupt bacterial and mammalian membranes, a large range of hydrophobic monomers have been tested to improve selectivity.[52] For instance, Kuroda and co-workers systematically investigated the impact of hydrophobic groups of binary copolymers on hemolysis and found that hemolytic activity increased as the hydrophobicity increased. To rationalize this effect, Kuroda[30,47] estimated partition coefficients (i.e., log *P*) by counting the number of carbon atoms in the side chains and found that high hemolytic activity was associated with a high log *P* value. Effectively, log *P* characterizes the hydrophobicity of a molecule using two immiscible layers, *n*-octanol and water,[53,54] and can indicate a preference for lipid-like membranes.

Inspired by Kuroda's work on binary copolymers,[30] this study aimed to evaluate the effect of the hydrophobic group of ternary copolymers and develop a predictive tool for screening the bioactivity of ternary copolymers prior to polymer preparation. To accomplish this goal, calculated log *P* values (*C* log *P*) of oligomeric models were utilized as a measure of the amphiphilic balance by accounting for the hydrophobic contribution of the polymer backbone as well as features of the side chains such as hybridization, branching, and number of carbon atoms. Using a library of eight hydrophobic monomers, we synthesized a library of 36 statistical amphiphilic ternary copolymers via reversible addition−fragmentation chain transfer (RAFT) polymerization[55,56] to systematically evaluate the copolymer composition, degree of polymerization (DP_n), hydrophobic monomer carbon length (5, 7, and 9 carbons), and chain type (cyclic, aromatic, linear, or branched) of the hydrophobic monomer on antimicrobial and hemolytic activity. Combining the data from this study with previous work,[33,57,58] an optimal *C* log *P* window for the prediction of antimicrobial activity and biocompatibility for ternary copolymers was determined.

MATERIALS AND METHODS

Materials. Ethylenediamine (Sigma-Aldrich, ≥99%), amylamine (Sigma-Aldrich), isopentylamine (Sigma-Aldrich, 99%), heptylamine (Sigma-Aldrich, 99%), *N*-propylbutylamine (Sigma-Aldrich, 98%), cycloheptylamine (Sigma-Aldrich, 99%), cyclohexanemethylamine (Sigma-Aldrich, 98%), nonylamine (Sigma-Aldrich, 98%), di-*tert*-butyl dicarbonate (Sigma-Aldrich, 99%), acryloyl chloride (Merck, ≥96%), *N*-hydroxyethyl acrylamide (HEAm) (Sigma-Aldrich, 97%), triethylamine (TEA) (Scharlau, 99%), trifluoroacetic acid (TFA) (Sigma-Aldrich, 99%), RAFT agent (2-(*n*-butyltrithiocarbonate)-propionic acid (BTPA), chloroform (Merck), dichloromethane (DCM) (Merck), tetrahydrofuran (THF) (Merck), diethyl ether, (Merck), hexane (Merck), dimethyl sulfoxide (DMSO) (Merck), *N*,*N*′-dimethylacetamide (DMAc) (Sigma-Aldrich), and 5,10,15,20-tetraphenyl-21*H*,23*H*-porphine zinc (ZnTPP) (Sigma-Aldrich) were used as received. Deionized (DI) water was produced by a Milli-Q water purification system and had a resistivity of 17.9 mΩ/cm.

Synthesis of Monomers. *Synthesis of Cationic Monomer: tert-Butyl (2-Acrylamidoethyl) Carbamate.* *tert*-Butyl (2-acrylamidoethyl)carbamate (Boc-AEAm) was prepared according to a previously reported procedure.[58] Ethylenediamine (0.33 mol) was dissolved in chloroform (400 mL). 0.03 mol of di-*tert*-butyl dicarbonate dissolved in 100 mL of chloroform was added dropwise to this solution over 4 h at 0 °C while stirring and then the reaction was continued overnight at room temperature. After filtering the white precipitate, the organic phase was washed with 200 mL of DI water six times and then dried using $MgSO_4$. Solids were separated by filtration, and the chloroform was evaporated resulting in a pale-yellow oil product, which was used in the next step.

THF (100 mL) was added to dissolve the obtained oil. TEA (1.2 equiv) and acryloyl chloride (1.1 equiv) were added dropwise to the solution at 0 °C with N_2 bubbling. The reaction mixture was then stirred at room temperature for 2 h. THF was then removed by rotary evaporation. The crude product was then dissolved in chloroform (150 mL) and washed against 0.1 M HCl solution (1 × 75 mL), saturated $NaHCO_3$ (1 × 75 mL), brine (1 × 75 mL), and DI water (1 × 75 mL). The organic phase was dried using $MgSO_4$ and filtered, and the remaining solvent was removed by rotary evaporation. The product was further purified by repeated precipitation steps in hexane to yield the Boc-protected monomer as a fine white powder, which was dried *in vacuo*. The yield for the monomer was 38 mol %.

Synthesis of Hydrophobic Monomers. A standard procedure was employed for the synthesis of eight hydrophobic monomers (*N*-

https://dx.doi.org/10.1021/acs.biomac.0c01320
Biomacromolecules XXXX, XXX, XXX−XXX

Table 1. *C* log *P* of Homopolymers with a Total DP_n of 10

		hydrophobic polymer							
cationic polymer	hydrophilic polymer	I	P	H	Pb	Cx	Cp	B	N
−6.18	−6.92	16.21	17.51	28.09	27.29	22.85	22.25	14.97	38.67

isopentylacrylamide, *N*-pentylacrylamide, *N*-heptylacrylamide, *N*-propylbutylacrylamide, *N*-(cycloheptyl)acrylamide, *N*-(cyclohexylmethyl)acrylamide, *N*-benzylacrylamide, and *N*-nonylacrylamide) from their corresponding amines.

Briefly, the specified amount of amine (either amylamine, isopentylamine, heptylamine, *N*-propylbutylamine, cycloheptylamine, *N*-cyclohexanemethylamine, *N*-benzylamine or *N*-nonylamine; 1 equivalent) was dissolved in THF with a ratio of 6 mL of THF per 1 mmol amine. TEA (1.2 equiv) and acryloyl chloride (1.2 equiv) were then added to this solution in a dropwise manner at 0 °C with N_2 bubbling. The mixture was stirred overnight at room temperature. The byproducts were filtered, and the solvent was removed by rotary evaporation. The crude product was dissolved in chloroform (1.5 times of THF volume) and then washed sequentially with 0.1 M HCl, saturated $NaHCO_3$, brine, and DI water using half of the chloroform volume for each wash. The organic phase was dried with $MgSO_4$ and basic Al_2O_3 and filtered to remove solids. Finally, the solvent was removed by rotary evaporation to yield the monomer. The yields for the monomers were between 55 and 76%.

Synthesis of Polymers. The statistical copolymers were synthesized using a slight modification of the general one-pot protocol reported previously.[33] Briefly, stock solutions of a monomer were prepared with a concentration of 33 wt % in DMSO. ZnTPP was dissolved in DMSO at a concentration of 1 mg mL^{-1}. RAFT agent BTPA was added to a 4 mL glass vial in an amount corresponding to the targeted degree of polymerization (100, 40, and 20 DP_n) and dissolved in DMSO. Monomer stock solutions were added into the vial to a final monomer concentration of 25 wt % in DMSO. The ZnTPP photocatalyst was added at 100 ppm to the monomer. The vial was sealed with a rubber septum and the headspace was degassed with N_2 for 10 min in an ice-water bath. The vial was then placed under a green LED light (λ = 530 nm) for 20 h to produce the Boc-protected copolymers. Finally, the copolymers were analyzed with SEC and NMR to examine the monomer conversion and other characteristics. Then, the polymer was purified by precipitating in a diethyl ether/hexane mixture (4:1) or (3:7), followed by centrifugation (9000 rpm for 3 min). The precipitate was dissolved in acetone and reprecipitated twice more. The polymer was then dried *in vacuo* prior to Boc group removal.

Deprotection. TFA was used to remove Boc-protecting groups based on our group's previously reported protocol.[59] Briefly, a polymer was dissolved in DCM (~7 wt % polymer), followed by the addition of TFA (20 mol equivalent with respect to Boc groups). The mixture was stirred at room temperature for 3 h and precipitated into diethyl ether. The precipitate was isolated by centrifugation, dissolved in acetone, and reprecipitated twice more. The polymer was then dried *in vacuo* and NMR analysis was used to determine the removal of Boc-protective groups.

Characterization. *Characterization of Polymers in Aqueous Media.* Dynamic light scattering (DLS) and zeta-potential measurements were measured using a Malvern Zetasizer Nano ZS apparatus equipped with a He−Ne laser operated at λ = 633 nm and at a scattering angle of 173°. All polymers were measured at a concentration of 1 mg/mL in DI water and the bacteria culture media (Mueller−Hinton broth, MHB).

For absorbance measurements, 200 μL of MHB solutions without or with polymers (1 mg/mL) was added to a 96-well microplate. The absorbance of the polymers in MHB at 595 nm was then measured using a microtiter plate reader (FLUOstar Omega, BMG Labtech).

^{1}H NMR Spectroscopy. NMR spectroscopy was used to analyze polymer composition and conversion. All experiments were performed on a Bruker Avance III 300 MHz NMR spectrometer. All experiments were run with a gas flow across the probes at 535 L/h with sample spinning and at a temperature of 25 °C. Samples were dissolved in deuterated NMR solvents supplied by Cambridge Isotopes (DMSO-d_6) at concentrations of 10−20 mg mL^{-1}. Spectra were referenced to residual protons in the NMR solvent (DMSO-d_6: δ 2.50 ppm).

Size Exclusion Chromatography. SEC analysis was performed in DMAc [with 0.03% w/v LiBr and 0.05% 2,6-di-butyl-4-methylphenol (BHT)] at 50 °C and a flow rate of 1 mL/min) with a Shimadzu modular system comprising an SIL-10AD automatic injector, a Polymer Laboratories 5.0 μL bead-size guard column (50 × 7.8 mm) followed by four linear PL (Styragel) columns (10^5, 10^4, 10^3, and 500 c5) and an RID-10A differential refractive-index detector. The system was calibrated using poly(methyl methacrylate) standards with molecular weights from 200 to 10^6 g mol^{-1}. Polymer solutions of 3 mg/mL were prepared in the eluent and filtered through 0.45 μm filters prior to injection.

C log P of Polymer Calculation and the Length of the Pendant Group. Log *P* is the partition constant of a compound between *n*-octanol (hydrophobic phase) and water (hydrophilic phase). The calculated log *P* (*C* log *P*) is the log *P* value obtained by calculation using a medicinal or chemical program as opposed to by experiment. In this study, the *C* log *P* of copolymers was carefully determined by ChemDraw (version 18.1) and Chem3D (version 18.1) using two methods for accuracy. First, *C* log *P* was calculated by the following equation

$$C \log P = (Aa + Bb + Cc)/100 \quad (1)$$

where *A*, *B*, and *C* are *C* log *P* of the cationic homopolymer, hydrophilic homopolymer, and hydrophobic homopolymer, respectively; *a*, *b*, *c* is the target ratio of the cationic monomer, hydrophilic monomer, and hydrophobic monomer, respectively.

As confirmation, the structures of copolymers replicating the target chemical ratio were drawn and their *C* log *P*s were computed by ChemDraw and Chem3D software (Supporting Information, Scheme S1). The *C* log *P*s obtained by both methods were identical.

It is important to note that these *C* log *P* values were calculated with a DP_n of 10, and this may slightly vary for different DP_n values (Table 1).

Minimum Inhibitory Concentration. The minimum inhibitory concentration (MIC) of the prepared polymers was determined via the broth microdilution method in accordance with the Clinical and Laboratory Standards Institute (CLSI) guidelines. The bacterial strains tested included *P. aeruginosa* (*PA*) *PAO1* and *ATCC 27853*, *Escherichia coli* (*EC*) *K12*, and *S. aureus ATCC 29213*. Bacterial culture was grown overnight from a single colony in 10 mL of MHB at 37 °C with shaking at 180 rpm. A subculture was prepared from the overnight culture by diluting 100 μL in 10 mL of MHB and growing to mid-log phase (approximately 2.5 h) and then diluted to ca. 1 × 10^6 cells mL^{-1}. A twofold dilution series of 100 μL of polymers in MHB solution were added to a 96-well microplate, followed by the addition of 100 μL of the subculture suspension. The final concentration of bacteria in each well was ca. 5 × 10^5 cells mL^{-1}. Positive controls without polymer and negative controls without bacteria or polymer were also included. The plates were then incubated at 37 °C for 20 h to ensure sufficient growth of inhibited bacteria, and the absorbance at 595 nm was measured with a microtiter plate reader (FLUOstar Omega, BMG Labtech). Bacterial growth inhibition was calculated using the following equation

$$\% \text{ inhibition} = [1 - (A_S - A_{CN})/(A_{CP} - A_{CN})] \times 100 \quad (2)$$

where A_{CP} is the absorbance of the positive control (no polymer), A_{CN} is the absorbance of the negative control (MHB only), and A_S is the absorbance of the tested sample. MIC values were defined as the

https://dx.doi.org/10.1021/acs.biomac.0c01320
Biomacromolecules XXXX, XXX, XXX−XXX

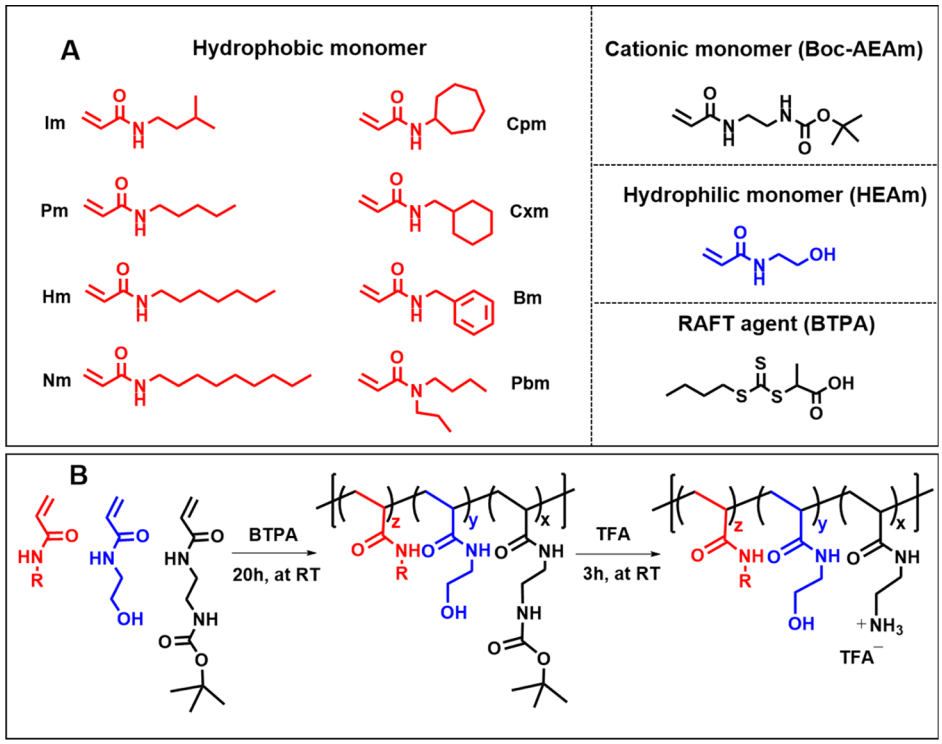

Figure 1. (A) Key reagents used in this study. Eight hydrophobic monomers: *N*-isopentylacrylamide (Im), *N*-pentylacrylamide (Pm), *N*-heptylacrylamide (Hm), *N*-butyl-*N*-propylacrylamide (Pbm), *N*-cycloheptylacrylamide (Cpm), *N*-(cyclohexylmethyl)acrylamide (Cxm), *N*-benzylacrylamide (Bm), and *N*-nonylacrylamide (Nm). Cationic monomer: Boc-AEAm. Hydrophilic monomer: hydroxyethyl acrylamide (HEAm). RAFT agent: BTPA. (B) Reaction scheme for the synthesis of antimicrobial polymers by PET-RAFT.

lowest concentration of the sample that showed no visible growth and inhibited cell growth by more than 90%. All assays included three replicates and were repeated in at least three independent experiments.

Membrane Potential Measurements. The membrane potential of the bacteria PA01 treated or untreated with polymers was measured based on the red-to-green fluorescence ratio of fluorophore $DiOC_2(3)$ in accordance with the method previously described by our group.[58] A subculture of PAO1 was prepared from an overnight culture in fresh MHB and allowed to grow to the mid log phase. Cells were then collected by centrifugation, resuspended, and adjusted to ca. 1×10^6 CFU mL^{-1} in M9 complete medium. A twofold dilution series of 50 μL of polymers in M9 complete medium were added into 96-well microplates (black with clear bottom), followed by the addition of 50 μL of $DiOC_2$ solution (30 μM in DI water) and 100 μL of the viable cells solution. The final concentration of bacteria in each well was ca. 5×10^5 cells mL^{-1}. The plates were incubated at 25 °C for 24 h. Membrane potential was determined using a microtiter plate reader (FLUOstar Omega, BMG Labtech) with 485 nm excitation and detection through 520 and 620 nm band-pass (ca. 10 nm bandwidth) filters. All assays included two replicates and were repeated in at least two independent experiments.

Hemolysis Studies. The hemolytic activity of polymers was determined using fresh sheep red blood cells (RBCs) in accordance with our group's previously reported protocol.[59] Briefly, RBCs were diluted 1:20 in PBS (pH 7.4), pelleted by centrifugation (1000*g*, 10 min), and washed three times in PBS. The RBCs were then resuspended to achieve 5% (v/v) in PBS. Different concentrations of polymers (150 μL) were prepared in sterilized tubes, followed by addition of the 5% RBC suspension (150 μL). Polymer concentrations tested were 2000, 1000, 500, 250, 125, 62.5, and 31.25 μg/mL. PBS buffer was used as a negative control, and Triton-X 100 (1% v/v in PBS) was used as a positive hemolysis control. Tubes were incubated at 37 °C for 2 h with 150 rpm shaking. Samples were then centrifuged (1000*g*, 8 min), 100 μL aliquots of supernatants were transferred into a 96-well microplate, and absorbance values were read at 485 nm using a microtiter plate reader (FLUOstar Omega, BMG Labtech). Hemolysis percentage was calculated using the following equation

$$\%\ \text{haemolysis} = (A_{\text{polymer}} - A_{\text{negative}})/(A_{\text{positive}} - A_{\text{negative}}) \times 100\% \quad (3)$$

where A_{polymer} is the absorbance of the polymer-treated supernatant, A_{negative} is the absorbance of the negative control, and A_{positive} is the absorbance of the positive control.

RESULTS AND DISCUSSION

In this study, a polymer library containing 36 ternary amphiphilic copolymers was prepared via photoinduced electron transfer-RAFT (PET-RAFT) polymerization by statistical copolymerization of eight different hydrophobic monomers with hydrophilic and cationic monomers (Figure 1). PET-RAFT was selected owing to its oxygen tolerance, which removes the need for stringent deoxygenation procedures. The hydrophilic and cationic monomers were fixed as HEAm and Boc-AEAm, respectively. Boc-AEAm was subsequently deprotected to reveal a primary amine. Hydrophobic monomers were prepared by amidation of acryloyl chloride in the presence of hydrophobic amine compounds (Supporting Information, Figures S1−S9). Based on the number of carbons (5, 7, or 9) used for the preparation of the hydrophobic monomer, the polymers were classified into three groups, namely, C5, C7, and C9, respectively. These groups were subdivided into eight families according to the type of hydrophobic monomer (Figure 1), namely, C5 group with *N*-isopentylacrylamide (I) and *N*-pentylacrylamide (P); C7 group with *N*-heptylacrylamide (H), *N*-butyl-*N*-propylacrylamide (Pb), *N*-cycloheptylacrylamide (Cp), *N*-

https://dx.doi.org/10.1021/acs.biomac.0c01320
Biomacromolecules XXXX, XXX, XXX−XXX

Table 2. Length of the Pendant Group

Pendant group	Structure of Pendant group	Length of pendant group (Å) [a,b]
Cationic monomer	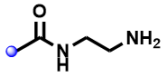	4.9
Hydrophilic monomer	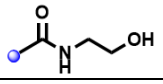	4.8
Im	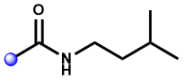	6.2
Pm	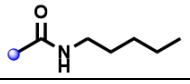	7.4
Hm	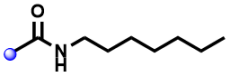	9.9
Pbm	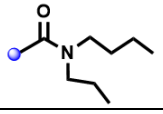	5
Cpm	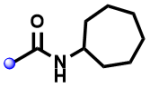	5.4
Cxm	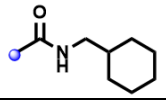	6.1
Bm	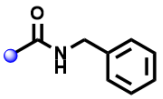	6.3
Nm	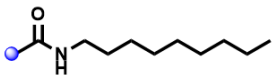	12.4

[a]The measurement was based on Chem3D software. [b]The length was measured from the carbonyl group carbon to the end group.

(cyclohexylmethyl)acrylamide (Cx), and *N*-benzylacrylamide (B); and C9 group with *N*-nonylacrylamide (N). Polymers were named as FD-RlRb where the *F* value corresponds to the family (I, P, H, Pb, Cp, Cx, B, or N); D to the targeted DP_n (i.e., 20, 40, or 100); Rl and Rb to the targeted molar composition of the hydrophilic monomer (HEAm) and hydrophobic monomer, respectively. The targeted composition of the cationic monomer was fixed at 50% for all polymers and, therefore, this description was not included in the nomenclature.

Characterization. All the copolymers prepared by PET-RAFT polymerizations were analyzed by SEC and proton nuclear magnetic resonance spectroscopy (^{1}H NMR) analysis to determine the molecular weight, dispersity, copolymer composition, and monomer conversion. The molecular weight distribution of all Boc-protected polymers was narrow as demonstrated by dispersity ($Đ$) values in the range of 1.06−1.17, which indicated good control of the polymerizations (Table 3). The number molecular weight (M_n) was estimated by SEC and ^{1}H NMR with good agreement between theoretical M_n and experimental values. ^{1}H NMR analysis of polymer mixtures prior to purification showed the near complete disappearance of vinyl proton signals at 5.5 and 6.3 ppm, indicating that monomer conversions were over 99% for all prepared polymers (Supporting Information, Figure S12). More importantly, ^{1}H NMR analysis of purified polymers exhibited good agreement between the monomer molar feed ratio and the purified copolymer composition (Supporting Information, Figures S12−S47). In the final step of copolymer preparation, the Boc groups were deprotected with TFA at room temperature overnight. The absence of the signal at 6.8 ppm (attributed to urethane group protons) and 1.4 ppm (attributed to *tert*-butyl group protons) in the ^{1}H NMR spectra of the polymers confirmed the successful removal of the Boc-protection group.

Representative polymers from each family were also characterized in aqueous media. All the characterized polymers had positive zeta potential (ζ) (10−35 mV) owing to the cationic charge of amino groups (Table 3). The presence of cationic amino and hydrophobic groups in antimicrobial polymers may induce the formation of so-called polymer−protein complexes (PPCs)[58] in biological media including the bacteria cell culture media MHB. To get an indication on the extent of PPC formation, DLS analysis, absorbance measure-

https://dx.doi.org/10.1021/acs.biomac.0c01320
Biomacromolecules XXXX, XXX, XXX−XXX

Table 3. Polymer Characterization by ^{1}H NMR, SEC, and DLS Analyses

family of polymers	polymer	number of carbons for hydrophobic monomers	type of hydrophobic monomer	target ratio of cationic/hydrophilic/hydrophobic	target DP_n	target M_n[a]	$M_{n,SEC}$[b]	$M_{n,MNR}$[c]	$Đ$[b]	D_h[d] (nm) in MHB	PDI[d] by DLS	ζ[d] (mV)	absorbance[e]
I-family	I40-1040	5	branched	50:10:40	40	7200	11,500	9700	1.1	173	0.1	22.5	0.1
	I40-1535	5	branched	50:15:35	40	7200	11,700	9200	1.06	-	-	18.9	nd
	I100-2030	5	branched	50:20:30	100	17,500	18,800	nd	1.17	-	-	nd	0.1
	I40-2030	5	branched	50:20:30	40	7100	8800	9200	1.13	-	-	27.9	0.07
	I20-2030	5	branched	50:20:30	20	3700	6700	9400	1.16	-	-	nd	0.07
	I40-2525	5	branched	50:25:25	40	7100	11,600	nd	1.11	-	-	nd	nd
	I40-3020	5	branched	50:30:20	40	6500	6800	nd	1.15	-	-	nd	nd
P-family	P40-1040	5	linear	50:10:40	40	7200	11,400	10,600	1.09	196	0.1	17.8	0.15
	P40-1535	5	linear	50:15:35	40	7200	12,200	9400	1.1	-	-	nd	nd
	P100-2030	5	linear	50:20:30	100	17,500	23,200	22,400	1.06	-	-	nd	nd
	P40-2030	5	linear	50:20:30	40	7100	11,400	9300	1.13	-	-	34.5	0.08
	P20-2030	5	linear	50:20:30	20	3700	7000	3900	1.09	-	-	nd	nd
H-family	H100-2030	7	linear	50:20:30	100	18,300	20,800	22,300	1.12	278	0.5	27.1	0.85
	H40-2030	7	linear	50:20:30	40	7500	9900	6500	1.14	nd	nd	nd	nd
	H20-2030	7	linear	50:20:30	20	3900	5500	4900	1.14	nd	nd	nd	nd
	H40-2525	7	linear	50:25:25	40	7400	12,700	9700	1.09	nd	nd	nd	0.15
	H40-3020	7	linear	50:30:20	40	7300	12,400	9500	1.08	nd	nd	nd	nd
Pb-family	Pb40-2030	7	branched	50:20:30	40	7500	10,300	nd	1.12	nd	nd	nd	nd
	Pb40-2525	7	branched	50:25:25	40	7400	11,300	nd	1.1	nd	nd	nd	nd
	Pb40-3020	7	branched	50:30:20	40	7300	11,900	nd	1.1	191	0.2	11.8	nd
Cp-family	Cp100-2030	7	cyclic	50:20:30	100	18,300	17,400	nd	1.08	291	0.1	nd	0.49
	Cp40-2030	7	cyclic	50:20:30	40	7500	7400	9300	1.11	262	0.1	27.8	0.37
	Cp20-2030	7	cyclic	50:20:30	20	3800	3800	4200	1.16	295	0.1	nd	0.34
	Cp40-2525	7	cyclic	50:25:25	40	7300	11,100	8100	1.08	nd	nd	nd	0.13
Cx-family	Cx100-2030	7	cyclic	50:20:30	100	18,300	17,600	23,800	1.09	339	0.2	nd	0.57
	Cx40-2030	7	cyclic	50:20:30	40	7500	8400	8700	1.1	353	0.3	10.6	0.54
	Cx20-2030	7	cyclic	50:20:30	20	3800	4300	4400	1.15	nd	nd	nd	nd
	Cx40-2525	7	cyclic	50:25:25	40	7300	11,400	7400	1.06	190	0.1	nd	nd
B-family	B40-1040	7	aromatic	50:10:40	40	7600	11,700	nd	1.11	nd	nd	nd	nd
	B40-1535	7	aromatic	50:15:35	40	7500	11,900	nd	1.1	nd	nd	nd	nd
	B100-2030	7	aromatic	50:20:30	100	18,100	23,400	nd	1.13	nd	nd	nd	nd
	B40-2030	7	aromatic	50:20:30	40	7400	11,200	nd	1.16	nd	nd	10.1	nd
	B20-2030	7	aromatic	50:20:30	20	3800	7000	nd	1.14	143	0.1	nd	0.09
N-family	N40-2030	9	linear	50:20:30	40	7800	11,400	9800	1.09	494	0.4	35.8	1.21
	N40-3020	9	linear	50:30:20	40	7500	12,900	8500	1.08	nd	nd	nd	nd
	N40-3515	9	linear	50:35:15	40	7300	12,700	nd	1.08	267	0.1	nd	0.22

[a]Theoretical molecular weight calculated using feed ratios and full monomer conversion (see the Supporting Information) before Boc-deprotection. [b]Determined via SEC analysis of copolymers before Boc-deprotection in the DMAc solvent. [c]Molecular weight calculated by NMR using the experimental copolymer composition in the copolymers (see the Supporting Information for additional information). [d]Determined by the Malvern Zetasizer Nano ZS apparatus after Boc-deprotection at a concentration of 1 mg/mL. [e]Determined at 595 nm in MHB after Boc-deprotection at a concentration of 1 mg/mL. (-) no aggregate. (nd)-not determined.

https://dx.doi.org/10.1021/acs.biomac.0c01320
Biomacromolecules XXXX, XXX, XXX−XXX

ments at 595 nm, and visual inspections were performed in both DI water and MHB (Table 3 and Supporting Information Figure. S48). In DI water, no turbidity was observed for any polymer (1 mg/mL) and all polymers were poorly detected by DLS, showing that the polymer was completely soluble at the given concentration without colloid formation. However, in MHB, some polymers formed PPCs[58] as evidenced by the detection of particles by DLS and absorbance measurements and the turbidity of the solutions observed visually. PPC formation occurs from the interaction of cationic groups with proteins and can lead to reduced antimicrobial activity as the cationic groups are prevented from complexing with the anionic bacterial membranes.[58,60] Group C5 (I/P families) generally did not form PPCs except for those polymers with a very low hydrophilic/hydrophobic ratio (I/P40-1040), whereas groups C7 and C9 did. The C7/9-polymers interacted rapidly with protein in MHB to form uniform PPCs, as indicated by the turbidity of polymers in MHB and detection of large particles by DLS. Notably, the C9 group polymer, N40-2030, formed the largest PPCs with an average hydrodynamic diameter (D_h) value of 494 nm. The D_h of PPC was reduced to 267 nm with a decrease in hydrophobic monomer ratio (N40-3515). This observation suggests that both overall hydrophobicity (C log P) and the chain length of the polymer have an impact on PPC formation. This is consistent with previous research from our group, which showed that increasing hydrophilic balance reduced PPC formation and improved antimicrobial activity.[58]

Bioactivity. *Antimicrobial Activity.* The antimicrobial activity of the polymers was evaluated by determining the MIC, which is the lowest concentration of the polymer that inhibits visible growth, of four bacterial strains: three Gram-negative strains, *P. aeruginosa* (*PA*) *PAO1* and *ATCC 27853*, *E. coli* (*EC*) *K12*; and a Gram-positive bacteria, *S. aureus ATCC 29213*.

As previously mentioned, antimicrobial polymers kill bacteria via membrane disruption.[16−20] These ternary amphiphilic polymers contain cationic, hydrophobic, and hydrophilic groups and each of these components performs a specific function. The cationic groups interact with the anionic bacterial membrane via electrostatic interaction, which not only enables the adsorption of polymers onto the anionic bacterial membrane but also affects the integrity of the cell membrane, interfering with the transport of compounds through the membrane.[16,18,20] Owing to its pivotal function, the cationic monomer usually comprises 50% of the molar composition of antimicrobial polymers. The interaction between the cationic groups and the cell membrane induces the polymer to adopt a globally amphiphilic conformation,[61] allowing the hydrophobic groups to insert into the membrane, leading to its disruption and cell death.[43] Finally, the hydrophilic groups reduce undesired protein complexation and hemolysis, thereby maintaining the antimicrobial activity of the polymers and conferring biocompatibility.[45,58,59] We first considered the MIC of our polymers against the different bacterial strains. Consistent with the findings of our group's previous research,[33,58,59] the polymers showed much higher antimicrobial activity against Gram-negative than against Gram-positive bacteria (Tables 4 and 5). The majority of polymers did not reach MICs against Gram-positive bacteria (*SA*) at any of the concentrations tested (MIC ≥ 256 μg/mL), whereas MICs varied from 16 to 256 μg/mL against Gram-negative bacteria depending on the polymer family, the DP_n, and the copolymer composition. The difference in activity of the polymers against Gram-negative and Gram-positive bacteria can be attributed to the difference in structure of their cell walls. Both Gram-positive and Gram-negative cell walls contain peptidoglycan, a polymer comprising amino acid and sugar groups. Gram-positive cell walls contain multiple layers of peptidoglycan in a rigid cross-linked structure, which prevents penetration of large hydrophobic molecules.[62−65] In contrast, the cell walls of Gram-negative bacteria have a thin layer of loosely cross-linked peptidoglycan as well as an outer membrane with lipopolysaccharide molecules attached, providing potential anchoring sites for the cationic groups of the polymer.[33,62,66] The lack of an outer lipopolysaccharide layer and the thick highly cross-linked peptidoglycan layer restrict penetration of antimicrobial polymers into Gram-positive bacteria, thereby reducing their activity. Interestingly, some B-family polymers (the polymers prepared using *N*-benzylacrylamide as the hydrophobic monomer) were able to achieve MICs at DP_n = 20 and 40, suggesting that this family of polymers may be more suited for Gram-positive bacteria than others. The response to polymers was also slightly different within the Gram-negative group of bacteria (Table 4). *EC K12* appeared to be slightly more sensitive to most tested polymers than *PAO1* and *PA 27853*. A possible explanation for this may be the difference in the lipopolysaccharide structure in their outer membranes.[66−68] Therefore, the type of bacterial strain is an important factor that should be considered in designing antimicrobial polymers.

Next, we focused on the intrinsic elements of the copolymers. We first investigated the effect of molecular weight by varying the degree of polymerization (DP_n = 20, 40, and 100) on antimicrobial activity. For the Gram-positive bacteria, *SA*, we noted that shorter polymers with a DP_n of 20 had higher activity with copolymers, I20-2030, P20-2030, H20-2030, Cp20-2030, and Cx20-2030, exhibiting MICs of 256 μg/mL, whereas their higher molecular weight (M_n) counterparts did not reach an MIC (Table 4). This is attributed to the greater mobility of short polymers, which can more readily penetrate the thick peptidoglycan cell wall to reach and disrupt the inner membrane of Gram-positive bacteria.[64] Against Gram-negative bacteria, however, there was no obvious trend of antimicrobial activity linked to the DP_n (in our tested range). For instance, in the I and P-families, polymers with different DP_n had similar MICs against *EC K12*, whereas polymers with a DP_n of 40 exhibited the highest antimicrobial activity against *PA01*. In the Cp-family, Cp20 was the best performing polymer against *EC K12* (MIC of 16−32 μg/mL) and *PA01* (MIC of 32 μg/mL), but there was no significant difference within polymers in the group against *PA 27853*. In the B-family, B100 showed the highest antimicrobial activity against *PA 27853* and *EC K12*, but this was not the case for *PA01*. This is consistent with the findings of Lienkamp, Tew, and co-workers who used dye-leakage data to determine that synthetic mimics of antimicrobial peptides damaged bacterial membranes regardless of their molecular weight.[64]

The amphiphilic balance of polymers is a critical factor in initiating bacterial membrane disruption.[16,18,20] The hydrophobicity of a compound can be measured by the logarithm of the partition coefficient of *n*-octanol/water (log P).[53,54] Positive log P values correspond to a preference for the lipid phase, while negative values indicate water solubility. However, log P (and hydrophobicity) increases with increasing molecular weight and, as discussed above, molecular weight does not

https://dx.doi.org/10.1021/acs.biomac.0c01320
Biomacromolecules XXXX, XXX, XXX−XXX

Table 4. Antimicrobial Activity (MIC) of Polymers with Similar Molar Ratios of Monomer Types but Varying DP_n against *P. aeruginosa ATCC 27853 and PAO1, E. coli K12,* and *S. aureus ATCC 29213*

Family of polymers	Hydrophobic monomer (CLogP values for the monomer)	Polymer	DP_n	CLogP of representative oligomer[a]	MIC of polymer (μg/mL)[b]			
					PA01	PA 27853	EC K12	SA 29213
I-family	*N*-isopentylacrylamide (1.40)	I100-2030	100	0.39	32-64	32-64	32	> 256
		I40-2030	40		16-32	32-64	32	>256
		I20-2030	20		32	64-128	32	256
P-family	*N*-pentylacrylamide (1.53)	P100-2030	100	0.78	32-64	32-64	32-64	>256
		P40-2030	40		32	32-64	32-64	>256
		P20-2030	20		64	128	32-64	256
H-family	*N*-heptylacrylamide (2.59)	H100-2030	100	3.95	128	128	128	>256
		H40-2030	40		64	128	64	>256
		H20-2030	20		128	128	nd	256
Cp-family	*N*-cycloheptylacrylamide (2.01)	Cp100-2030	100	2.20	64	64-128	64	>256
		Cp40-2030	40		32-64	64	32	>256
		Cp20-2030	20		32	64-128	16-32	256
Cx-family	*N*-(cyclohexylmethyl)acrylamide (2.07)	Cx100-2030	100	2.38	64	64	64	>256
		Cx40-2030	40		32	32-64	32	>256
		Cx20-2030	20		32-64	64	16-32	256
B-family	*N*-benzylacrylamide (1.19)	B100-2030	100	0.05	64-128	64	128	>256
		B40-2030	40		64	64-128	256	256
		B20-2030	20		128	128-256	256	256

Higher efficacy

[a]*C* log *P* of the representative oligomer was calculated using a theoretical DP_n of 10 [ChemDraw (version 18.1 and 19.0) software]. [b]MIC values were determined using triplicate experiments.

correlate with antimicrobial activity for Gram-negative bacteria. We, therefore, hypothesized that a more relevant metric would be to calculate the log *P* for a representative oligomer model of each polymer. As the typical size of oligomeric models ranges from 5 to 20 units,[69] we employed 10 units.

Two of the most common computational strategies for calculating log *P* are atom-based (i.e., *A* log *P*) and fragment-based (i.e., *C* log *P*) methods.[53] In the atom-based approach, each atom contributes to the overall hydrophobicity depending on the type of atom, hybridization, and connection to other atoms. In contrast, fragment-based methods break a molecule into atoms and functional groups with a variety of correction factors to account for hydrogen bonding, unsaturation, and other features.[70] As most recent reports focus on *A* log *P*,[71] we hypothesize that *C* log *P* has underutilized potential. In this work, *C* log *P* values for a theoretical DP_n equal to 10 were verified by two methods [using ChemDraw (version 18.1 and 19.0) and Chem3D (version 18.1)] for accuracy.

As hydrophilic and cationic monomers were not varied in this work, the hydrophobicity of copolymers was solely influenced by the hydrophobic monomers and the monomer ratio in the copolymers. Therefore, we examined the feed ratio of the copolymer components and found that the antimicrobial activity was strongly dependent on the hydrophobic monomer content of the polymer. The general trend was that increasing the ratio of the hydrophobic monomer led to an increase in the antimicrobial activity (Table 5). However, we found an interesting exception with the polymers in the N-family. This is the family that has the longest carbon chain-length pendant group (9 carbons). Unlike other tested families, which have shorter chain-length hydrophobic groups, N-family polymers exhibited an increase in antimicrobial activity as the ratio of the hydrophobic monomer decreased. This difference in activity is potentially explained by the behavior of the N-family in MHB media. As discussed above, the N-family formed PPCs in MHB, which could have hindered the electrostatic interaction between the cationic groups and the bacteria membrane. The greater PPC formation was in the copolymer with the highest hydrophobic content (N40-2030) and lowest antimicrobial activity, whereas the less hydrophobic N40-3515 had lower PPC formation and a better antibacterial effect.

We also investigated polymers with the same composition but different hydrophobic monomers and found that for polymers with saturated chains and a similar DP_n and target molar ratio of components (***P40-2030***, ***I40-2030***, ***H40-2030***, ***Pb40-2030***, ***Cp40-2030***, ***Cx40-2030***, and ***N40-2030***), the antimicrobial activity reduced as the number of carbons of the hydrophobic pendant groups increased (i.e., group C9 had higher MIC values than C7 and C5). For polymers in the same group, the copolymers containing branched chain monomers showed better antimicrobial activity than those with linear chains. It is important to note that for the same number of carbons, a branched chain is shorter than a linear chain (Table 2). In the C5 group, the length of the Im (6.2 Å) is slightly shorter than that of the Pm (7.4 Å), and the MIC values of I40-1535 against Gram-negative bacteria were also slightly lower than the MIC values of P40-1535. In the C7 group, where the difference in chain length between the branched (Pbm, 5 Å) and the linear (Hm, 9.9 Å) monomers was larger, the difference in antimicrobial activity was also larger. For example, the MICs against *PAO1*, *PA 27853*, and *EC K12* for Pb40-2030 were 32, 32−64, and 16−32 μg/mL, respectively, whereas those for H40-2030 were 64, 128, and 64 μg/mL, respectively (Table 5).

As detailed above, structural compatibility of the chosen monomers is a critical factor for optimizing antimicrobial

https://dx.doi.org/10.1021/acs.biomac.0c01320
Biomacromolecules XXXX, XXX, XXX−XXX

Table 5. Antimicrobial Activity (MIC) of 40-DP$_n$ Polymers with Varying Hydrophobic Monomers and Monomer Feed Ratios against *P. aeruginosa ATCC 27853* and *PAO1*, *E. coli K12*, and *S. aureus ATCC 29213*

Family of polymer	Hydrophobic monomer (CLogP)	Polymer	Monomer Ratio[a]	CLogP of representative oligomer[b]	MIC of polymer (μg/mL) [c]			
					PA01	PA 27853	EC K12	SA 29213
I-family	*N*-isopentylacrylamide (1.40)	I40-1040	50:10:40	2.70	16	16-32	16	>256
		I40-1535	50:15:35	1.55	16	16-32	16	>256
		I40-2030	50:20:30	0.39	16-32	32-64	32	>256
		I40-2525	50:25:25	-0.77	256	>256	128-256	>256
		I40-3020	50:30:20	-1.93	>256	>256	>256	>256
P-family	*N*-pentylacrylamide (1.53)	P40-1040	50:10:40	3.22	32	32	16	>256
		P40-1535	50:15:35	2.00	32	32	16	>256
		P40-2030	50:20:30	0.78	32	32-64	32-64	>256
H-family	*N*-heptylacrylamide (2.59)	H40-2030	50:20:30	3.95	64	128	64	>256
		H40-2525	50:25:25	2.2	64	64	64	>256
		H40-3020	50:30:20	0.45	64-128	128-256	128	>256
Pb-family	*N*-butyl-*N*-propylacrylamide (2.37)	Pb40-2030	50:20:30	3.70	32	32-64	16-32	>256
		Pb40-2525	50:25:25	2.00	32-64	32-64	32-64	>256
		Pb40-3020	50:30:20	0.29	64	128	128-256	>256
Cp-family	*N*-cycloheptylacrylamide (2.01)	Cp40-2030	50:20:30	2.20	32-64	64	32	>256
		Cp40-2525	50:25:25	0.74	32-64	32-64	16-32	>256
Cx-family	*N*-(cyclohexylmethyl)acrylamide (2.07)	Cx40-2030	50:20:30	2.38	32	32-64	32	>256
		Cx40-2525	50:25:25	0.89	32-64	64	16-32	>256
B-family	*N*-benzylacrylamide (1.19)	B40-1535	50:15:35	1.11	32-64	64	64-128	>256
		B40-1040	50:10:40	2.23	16-32	32	32	256
		B40-2030	50:20:30	0.05	64	64-128	256	256
N-family	*N*-nonylacrylamide (3.65)	N40-2030	50:20:30	7.13	>256	>256	>256	>256
		N40-3020	50:30:20	2.57	128-256	256	128-256	>256
		N40-3515	50:35:15	0.29	128-256	256	128-256	>256

Higher efficacy

[a]Ratio of cationic/hydrophilic/hydrophobic monomer. [b]*C* log *P* of representative oligomer was calculated using a theoretical DP$_n$ = 10. [c]MIC values were determined using triplicate experiments.

activity. Achieving a compatible length between components plays a pivotal role in modulating the polymer−membrane interactions and concomitant activity. Furthermore, the cationic group should not be hindered by complexation with proteins to maximize its availability toward the anionic membrane of bacteria. Amongst the hydrophobic monomers tested, the I-monomer was the most compatible with the chosen cationic and hydrophilic monomers because of the lack of protein complexation in aqueous media, as indicated by polymers I40-1535 and I40-1040, which showed the highest antimicrobial activity in the library tested.

To further elucidate the relationship between polymer structure and antimicrobial activity, we conducted membrane potential measurements on bacteria treated with representative polymers of each group to determine the degree of membrane disruption.[58] In a series of seminal papers, Tew and Wong[72−76] demonstrated that synthetic mimics of antimicrobial peptides exhibited their antimicrobial efficacy by inducing curvature (pore formation) in bacterial membranes containing negative intrinsic curvature (NIC) lipids, such as phosphatidylethanolamine (PE). If our polymers acted by a similar mechanism, we would expect to see the greatest loss of membrane potentials recorded for polymers with the lowest MICs. Membrane potentials were detected in PA01 cells with a carbocyanine dye, 3,3′-diethyloxacarbocyanine iodide, which exhibits green fluorescence (520 nm) in cell media but shifts toward red emission (620 nm) as the dye accumulates in bacteria cytosol (viable bacteria). The lower the ratio of red-to-green fluorescence, the greater the loss of membrane potential and, therefore, the greater the extent of membrane disruption. Figure 2 shows the ratio of red-to-green fluorescence for PAO1 cells treated with different concentrations of polymers. Untreated cells (without any polymer) displayed a red-to-green fluorescence ratio (∼0.94), which is considered normal for bacterial cells. Consistent with our antimicrobial tests, among the eight representatives from each family, I40-2030 and P40-2030, which showed the lowest MICs, exhibited the lowest red-to-green ratios, whereas N40-2030, which was inactive against PA01 at all concentrations tested, exhibited the highest red-to-green ratio. This is consistent with the findings of Tew and Wong and suggests that the hydrophobic monomers in the I and P polymers have greater affinity for NIC lipids, such as PE, than the more hydrophobic monomers found in other polymer families.

Finally, we analyzed the correlation between the *C* log *P* of representative oligomers of each family and their antimicrobial

https://dx.doi.org/10.1021/acs.biomac.0c01320
Biomacromolecules XXXX, XXX, XXX−XXX

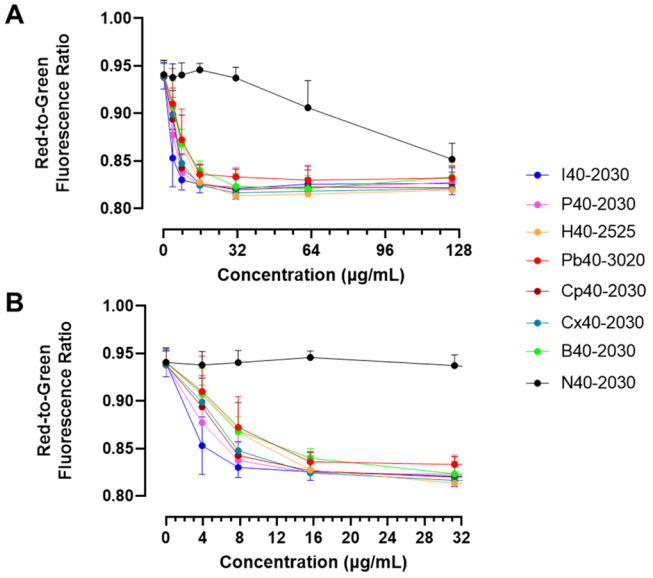

Figure 2. Cytoplasmic membrane potential measurements indicating the red-to-green fluorescence ratio of cells treated with representative antimicrobial polymers. (A) Large range of the tested concentration and (B) small range of the tested concentration.

activity. To reduce confounding factors, we compared the antimicrobial activity of representatives from all families with consistent DP_n of 40. To clarify the influence of the *C* log *P* on antimicrobial activity, we also varied the ratio of hydrophilic and hydrophobic monomers in the formulations. As a result, we found that the *C* log *P* should be in the range 0−6 for optimal bactericidal activity (Table 5). To confirm this range, we calculated *C* log *P* values for statistical antimicrobial polymers from our group's previous work[33,57,58] and plotted them against the reported MIC values for *PAO1* along with the results from the present study (Figure 3, Supporting Information, Table S2). Consistent with our findings, the antimicrobial activity of these copolymers (MIC values) correlated with the *C* log *P* values. Whereas there was some variation in activity versus *C* log *P*, all polymers showing poor antimicrobial activity (MIC > 128 μg/mL) had *C* log *P* values outside the range 0−6. These trends can be used as a simple tool to pre-estimate the antimicrobial activity against Gram-negative bacteria (*PAO1*) in designing new antimicrobial polymers. However, to improve the accuracy, in addition to the *C* log *P* value, other parameters should be considered. For instance, to maximize antimicrobial activity, the molar ratio of a hydrophobic monomer should be above 20% and, as discussed above, the structural compatibility and cationic/hydrophobic balance are critical.

Hemolytic Activity. The hemolytic activity against fresh sheep blood cells (erythrocytes) was used to assess the mammalian cell compatibility of our membrane-active antimicrobial polymers. Numerous studies have reported that hydrophobicity plays a key role in inducing hemolysis,[30,77,78] reducing biocompatibility of antimicrobial polymers. In this study, our aim was to gain a more detailed understanding of this concept and determine how hemolysis is affected by the overall hydrophobicity as well as the influence of various factors, including the nature of hydrophobic monomers, the monomer ratio within copolymers, and the overall molecular weight.

To assess the effect of the monomer ratio, we compared the hemolytic activity of polymers within each family. As can be seen from Table 6, the hydrophobic monomer content of the copolymer was directly proportional to both the calculated *C* log *P* of the representative oligomer and the hemolysis induced. For the C5 group, which includes the I- and P-families, substantial hemolysis was observed when the proportion of hydrophobic monomer reached 40%, whereas for the C7 group (except for the B-family) and the C9 group, hemolysis occurred when the proportion was only 30% (Table 6). For the more highly hydrophobic monomers in the C7 and C9 groups, a lower proportion of the hydrophobic monomer was required to achieve a high *C* log *P* for the representative oligomer and subsequently higher hemolytic activity. In contrast to bacterial cells where the interaction between cationic groups and anionic membranes is critical,[16,18,20,79]

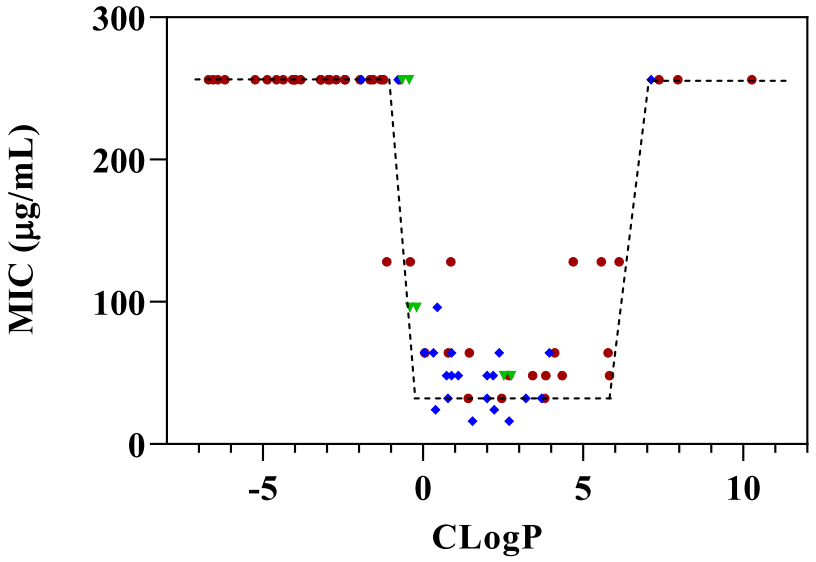

Figure 3. Correlation between *C* log *P* of polymers and their MIC against *PA01*. MIC > 128 μg/mL was plotted as 256 μg/mL for ease of viewing. Note: brown ● polymers from ref 33; green ▼ polymers from refs 57 and 58; blue ♦ polymers in the present study. *C* log *P* was calculated using a theoretical DP_n of 10 (ChemDraw (version 18.1 and 19.0) software.

https://dx.doi.org/10.1021/acs.biomac.0c01320
Biomacromolecules XXXX, XXX, XXX−XXX

Table 6. Hemolytic Activity of Polymers

Family of polymers	Polymer	Monomer Ratio[a]	CLogP of representative oligomer[b]	HC_{50} (μg/mL)
I-family	I40-1040	50:10:40	2.70	141.5 ± 5.9
	I40-1535	50:15:35	1.55	> 2000
	I100-2030	50:20:30	0.39	> 2000
	I40-2030	50:20:30		> 2000
	I20-2030	50:20:30		> 2000
	I40-2525	50:25:25	-0.77	No haemolysis
	I40-3020	50:30:20	-1.93	No haemolysis
P-family	P40-1040	50:10:40	3.22	86.9 ± 9.1
	P40-1535	50:15:35	2.00	~2000
	P100-2030	50:20:30	0.78	> 2000
	P40-2030	50:20:30		> 2000
	P20-2030	50:20:30		> 2000
H-family	H100-2030	50:20:30	3.95	149 ± 87.3
	H40-2030	50:20:30		1150.0 ± 392.2
	H20-2030	50:20:30		574.4 ± 209.2
	H40-2525	50:25:25	2.2	> 2000
	H40-3020	50:30:20	0.45	> 2000
Pb-family	Pb40-2030	50:20:30	3.70	523.4 ± 149.4
	Pb40-2525	50:25:25	2.00	>2000
	Pb40-3020	50:30:20	0.29	No haemolysis
Cp-family	Cp100-2030	50:20:30	2.20	75 ± 45.4
	Cp40-2030	50:20:30		123.0 ± 12.6
	Cp20-2030	50:20:30		190.2 ± 58.6
	Cp40-2525	50:25:25	0.74	~ 2000
Cx-family	Cx100-2030	50:20:30	2.38	140.2 ± 21.1
	Cx40-2030	50:20:30		130.7 ± 20.2
	Cx20-2030	50:20:30		169.1 ± 71.4
	Cx40-2525	50:25:25	0.89	~2000
B-family	B40-1040	50:10:40	2.23	961 ±425.3
	B40-1535	50:15:35	1.11	> 2000
	B100-2030	50:20:30	0.05	> 2000
	B40-2030	50:20:30		> 2000
	B20-2030	50:20:30		> 2000
N-family	N40-2030	50:20:30	7.13	257.1 ± 36.8
	N40-3020	50:30:20	2.57	> 2000
	N40-3515	50:35:15	0.29	No haemolysis

Higher haemolysis

[a]Ratio of cationic/hydrophilic/hydrophobic monomer. [b]*C* log *P* of representative oligomer was calculated based on a theoretical DP_n of 10.

binding of antimicrobial polymers to the more neutral mammalian cell membranes[16,79] is believed to be primarily owing to the partitioning of the hydrophobic groups from the aqueous phase to the hydrophobic regions of the lipid layers.[30,79,80]

To investigate the effect of molecular weight of copolymers on hemolytic activity, we synthesized polymers from I, P, H, Cx, Cp, and B monomer families with DP_n values of 20, 40, and 100 and examined their hemolytic activity. The results revealed no clear trends in the hemolytic activity of polymers with different DP_n within each tested family (Table 6). As mentioned above, the hydrophobicity of polymers is known to increase with DP_n, so, as with antimicrobial activity, the relationship between hemolytic activity and hydrophobicity is nuanced.

Next, we investigated the hydrophobic monomer structure by comparing representatives from eight families, namely, I40-2030, P40-2030, H40-2030, Pb40-2030, Cx40-2030, Cp40-2030, B40-2030, and N40-2030, with the same DP_n (40) and polymer composition (molar ratio of cationic/hydrophilic/hydrophobic equal to 50:20:30). We found that the structure of the hydrophobic monomer had a significant impact on the hemolytic activity. In general, increasing the carbon length of the pendant hydrophobic group correlated with an increase in the *C* log *P* of the hydrophobic monomer, thereby increasing the *C* log *P* of the copolymers, which led to a rise in hemolysis (Table 6, Supporting Information, Figure S49).

Comparing the activity of the polymers in the C7 group, which include linear, cyclic, and aromatic hydrophobic monomers, allowed us to also investigate the effects of the structure on hemolytic activity. The aromatic B-family had the

https://dx.doi.org/10.1021/acs.biomac.0c01320
Biomacromolecules XXXX, XXX, XXX−XXX

lowest hydrophobicity (*C* log *P* of Bm = 1.19) owing to the polarizability of the pi electrons in the benzene ring and, in line with the general trend noted above, had the lowest hemolytic activity (Table 5, Supporting Information, Figure S49). In contrast, polymers in cyclic families (Cp and Cx), despite having lower *C* log *P* values than the acyclic polymers (Pb and H), had higher hemolytic activity (Table 6, Supporting Information, Figure S49). We speculate that the reason may be related to the interaction of the cyclic groups of the polymers with the tetracyclic ring system of cholesterol, which comprises approximately 25% of eukaryotic cell membranes.[81−83] The rigid ring structure of cholesterol stabilizes and strengthens the membrane bilayer and reduces its permeability[84] and, therefore, the presence of cholesterol in eukaryote membranes, but not in bacterial membranes, has been proposed as one of the reasons for the selective toxicity of AMPs.[85,86] However, further research is required to confirm if the cyclic groups are more likely to interact with cholesterol than other hydrophobic groups.

Finally, we compared the effect of the *C* log of the representative oligomers of the cationic amphiphilic statistical copolymers on hemolytic activity and antimicrobial activity. The general trend is summarized in Figure 4. Unlike

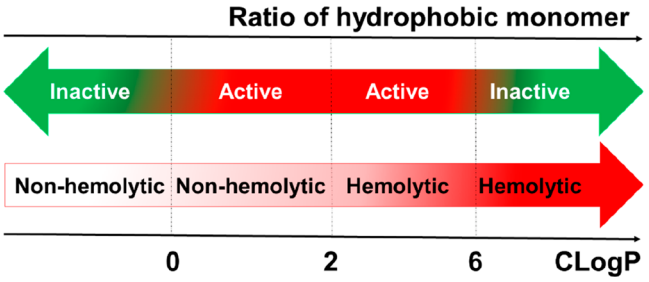

Figure 4. Correlation between *C* log *P* and bioactivity of the polymers. Note: *C* log *P* is of a representative oligomer calculated using a theoretical DP_n of 10 (ChemDraw (version 18.1 and 19.0) software.

antimicrobial activity, which is maximized when *C* log *P* is neither too low nor too high (see green two-directional arrow), favorable hemolytic activity occurs when *C* log *P* is at lower values (see the red one-directional arrow) (Figure 4). Notably, almost no hemolysis was detected with polymers with a negative *C* log *P* value. By contrast, in our tested range, substantial hemolytic activity was observed for polymers with *C* log *P* of > 2, which tended to occur with a hydrophobic proportion of ≥30%. Consequently, the optimum range of *C* log *P* where polymers were active against bacteria without inducing hemolysis was between 0 and 2.

Finally, to validate our conclusion, we compared our predictive model with the experimental values obtained from three additional polymers, including two polymers with good activity against *PA01* and a third polymer with a poor antimicrobial activity (Table 7). Encouragingly, the experimental and predicted MIC and hemolysis values are in good agreement, which confirms that our approach can be utilized to guide the design of new antimicrobial polymers.

CONCLUSIONS

A library of 36 statistical amphiphilic polymers was successfully synthesized using a living/controlled radical polymerization technique and screened against four bacterial strains and sheep erythrocytes to examine antimicrobial activity and hemocompatibility, respectively. We systematically evaluated the monomer ratio, degree of polymerization (DP_n), hydrophobic monomer carbon length (5, 7, and 9 carbons), and chain type (cyclic, aromatic, linear, or branched) of the hydrophobic monomer on bacteriostatic activity and biocompatibility. The study revealed that minimizing hydrophobicity and hydrophobic content were key factors in controlling hemolysis, whereas optimizing antimicrobial activity was more complex. High antimicrobial activity required hydrophobicity that was neither too high nor too low, an appropriate cationic/hydrophobic balance, and structural compatibility between the chosen monomers. Furthermore, we developed a pre-experimental screening mechanism for future antimicrobial ternary copolymer design, finding that polymers with a *C* log *P* (hydrophobicity index) between 0 and 2 were most likely to have the best balance of high antimicrobial activity and low hemolytic activity and therefore had the best potential for experimental study. However, it should be noted that this value is only useful for initial screening and should be combined with other parameters, such as structural compatibility and cationic/hydrophobic balance, to optimize antimicrobial polymer design.

ASSOCIATED CONTENT

Supporting Information

The Supporting Information is available free of charge at https://pubs.acs.org/doi/10.1021/acs.biomac.0c01320.

Characterization of monomers (^{1}H NMR spectra of monomers: Boc-AEAm monomer, *N*-pentyl acrylamide, *N*-isopentyl acrylamide, *N*-heptyl acrylamide, *N*-(cyclo-

Table 7. Comparison of Predicted and Experimental Antimicrobial and Hemolytic Activity of Polymers

AEAm[a]	HEAm[a]	PEAm[a]	DP_n	CLogP of representative oligomer[b]	Predicted MIC against *PA01*	Experimental MIC against *PA01* [32]	Predicted haemolysis	Experimental haemolysis [32]
50	20	30	40	0.7				
70	0	30	40	0.9				
50	35	15	40	-2.9				

MIC > 128 μg/ml
MIC ≤ 128 μg/ml
Favourable haemolysis
No haemolysis

[a]Molar ratio of cationic monomer (AEAm: 2-aminoethylacrylamide), hydrophilic monomer (HEAM: 2-hydroxyethylacrylamide), and hydrophobic monomer (PEAm: phenylethyl acrylamide), respectively.[32] [b]*C* log *P* of the representative oligomer was calculated using a theoretical DP_n of 10. The polymer was predicted to have antimicrobial effect (MIC ≤ 128 μg/mL) if its *C* log *P* was 0−6. The polymer was predicted to induce no hemolysis, favorable hemolysis, or substantial hemolysis if its *C* log *P* was ≤0, 0−2, or ≥2, respectively.

https://dx.doi.org/10.1021/acs.biomac.0c01320
Biomacromolecules XXXX, XXX, XXX−XXX

heptyl) acrylamide, *N*-propyl butylacrylamide, *N*-(cyclohexylmethyl) acrylamide, *N*-benzyl acrylamide, *N*-nonyl acrylamide); kinetics studies of copolymerization of representative monomers; characterization of antimicrobial polymers, including ^{1}H NMR spectra, molecular weight distributions determined by GPC and calculations for polymer compositions; *C* log *P* calculation; characterization of polymers in aqueous medium; antimicrobial activity and *C* log *P*; and hemolytic activity versus polymer concentration (PDF)

AUTHOR INFORMATION

Corresponding Authors

Robert T. Mathers − *Department of Chemistry, Penn State University, New Kensington, Pennsylvania 15068, United States;* orcid.org/0000-0002-0503-4571; Email: rtm11@psu.edu

Cyrille Boyer − *Australian Centre for NanoMedicine, School of Chemical Engineering, The University of New South Wales, Sydney, New South Wales 2052, Australia;* orcid.org/0000-0002-4564-4702; Email: cboyer@unsw.edu.au

Authors

Pham Thu Phuong − *Australian Centre for NanoMedicine, School of Chemical Engineering, The University of New South Wales, Sydney, New South Wales 2052, Australia*

Susan Oliver − *Australian Centre for NanoMedicine, School of Chemical Engineering, The University of New South Wales, Sydney, New South Wales 2052, Australia*

Junchen He − *Australian Centre for NanoMedicine, School of Chemical Engineering, The University of New South Wales, Sydney, New South Wales 2052, Australia*

Edgar H. H. Wong − *Australian Centre for NanoMedicine, School of Chemical Engineering, The University of New South Wales, Sydney, New South Wales 2052, Australia;* orcid.org/0000-0001-5151-5045

Complete contact information is available at: https://pubs.acs.org/10.1021/acs.biomac.0c01320

Author Contributions

The manuscript was written through contributions of all authors. All authors have given approval to the final version of the manuscript.

Notes

The authors declare no competing financial interest.

REFERENCES

(1) Wright, G. D. Solving the Antibiotic Crisis. *ACS Infect. Dis.* **2015**, *1*, 80−84.

(2) Rex, J. H.; Eisenstein, B. I.; Alder, J.; Goldberger, M.; Meyer, R.; Dane, A.; Friedland, I.; Knirsch, C.; Sanhai, W. R.; Tomayko, J.; Lancaster, C.; Jackson, J. A Comprehensive Regulatory Framework to Address the Unmet Need for New Antibacterial Treatments. *Lancet Infect. Dis.* **2013**, *13*, 269−275.

(3) Wright, G. D. Antibiotic Adjuvants: Rescuing Antibiotics from Resistance. *Trends Microbiol.* **2016**, *24*, 862−871.

(4) Brogan, D. M.; Mossialos, E. A Critical Analysis of the Review on Antimicrobial Resistance Report and the Infectious Disease Financing Facility. *Glob. Health* **2016**, *12*, 8.

(5) Santajit, S.; Indrawattana, N. Mechanisms of Antimicrobial Resistance in Eskape Pathogens. *BioMed Res. Int.* **2016**, *2016*, 2475067.

(6) Kamaruzzaman, N. F.; Tan, L. P.; Hamdan, R. H.; Choong, S. S.; Wong, W. K.; Gibson, A. J.; Chivu, A.; Pina, M. d. F. Antimicrobial Polymers: The Potential Replacement of Existing Antibiotics? *Int. J. Mol. Sci.* **2019**, *20*, 2747.

(7) Cuthbert, T. J.; Hisey, B.; Harrison, T. D.; Trant, J. F.; Gillies, E. R.; Ragogna, P. J. Surprising Antibacterial Activity and Selectivity of Hydrophilic Polyphosphoniums Featuring Sugar and Hydroxy Substituents. *Angew. Chem., Int. Ed.* **2018**, *57*, 12707−12710.

(8) Hisey, B.; Ragogna, P. J.; Gillies, E. R. Phosphonium-Functionalized Polymer Micelles with Intrinsic Antibacterial Activity. *Biomacromolecules* **2017**, *18*, 914−923.

(9) Al-Ahmad, A.; Laird, D.; Zou, P.; Tomakidi, P.; Steinberg, T.; Lienkamp, K. Nature-Inspired Antimicrobial Polymers—Assessment of Their Potential for Biomedical Applications. *PloS One* **2013**, *8*, No. e73812.

(10) Richards, S.-J.; Jones, A.; Tomás, R. M. F.; Gibson, M. I. Photochemical "in-Air" Combinatorial Discovery of Antimicrobial Co-Polymers. *Chem.—Eur. J.* **2018**, *24*, 13758−13761.

(11) Roy, D.; Knapp, J. S.; Guthrie, J. T.; Perrier, S. Antibacterial Cellulose Fiber Via Raft Surface Graft Polymerization. *Biomacromolecules* **2008**, *9*, 91−99.

(12) Phillips, D. J.; Harrison, J.; Richards, S.-J.; Mitchell, D. E.; Tichauer, E.; Hubbard, A. T. M.; Guy, C.; Hands-Portman, I.; Fullam, E.; Gibson, M. I. Evaluation of the Antimicrobial Activity of Cationic Polymers against Mycobacteria: Toward Antitubercular Macromolecules. *Biomacromolecules* **2017**, *18*, 1592−1599.

(13) Kuroki, A.; Sangwan, P.; Qu, Y.; Peltier, R.; Sanchez-Cano, C.; Moat, J.; Dowson, C. G.; Williams, E. G. L.; Locock, K. E. S.; Hartlieb, M.; Perrier, S. Sequence Control as a Powerful Tool for Improving the Selectivity of Antimicrobial Polymers. *ACS Appl. Mater. Interfaces* **2017**, *9*, 40117−40126.

(14) Zhang, L.-j.; Gallo, R. L. Antimicrobial Peptides. *Curr. Biol.* **2016**, *26*, R14−R19.

(15) Cardoso, M. H.; Oshiro, K. G. N.; Rezende, S. B.; Cândido, E. S.; Franco, O. L. Chapter Ten—The Structure/Function Relationship in Antimicrobial Peptides: What Can We Obtain from Structural Data?. In *Advances in Protein Chemistry and Structural Biology*, Donev, R., Ed.; Academic Press, 2018; Vol. *112*, pp 359−384.

(16) Zasloff, M. Antimicrobial Peptides of Multicellular Organisms. *Nature* **2002**, *415*, 389−395.

(17) Hancock, R. E. W.; Sahl, H.-G. Antimicrobial and Host-Defense Peptides as New Anti-Infective Therapeutic Strategies. *Nat. Biotechnol.* **2006**, *24*, 1551−1557.

(18) Santos, M.; Fonseca, A.; Mendonça, P.; Branco, R.; Serra, A.; Morais, P.; Coelho, J. Recent Developments in Antimicrobial Polymers: A Review. *Materials* **2016**, *9*, 599.

(19) Scott, R. W.; DeGrado, W. F.; Tew, G. N. De Novo Designed Synthetic Mimics of Antimicrobial Peptides. *Curr. Opin. Biotechnol.* **2008**, *19*, 620−627.

(20) Takahashi, H.; Caputo, G. A.; Vemparala, S.; Kuroda, K. Synthetic Random Copolymers as a Molecular Platform to Mimic Host-Defense Antimicrobial Peptides. *Bioconjugate Chem.* **2017**, *28*, 1340−1350.

(21) Ergene, C.; Palermo, E. F. Antimicrobial Synthetic Polymers: An Update on Structure-Activity Relationships. *Curr. Pharm. Des.* **2018**, *24*, 855−865.

(22) Tew, G. N.; Liu, D.; Chen, B.; Doerksen, R. J.; Kaplan, J.; Carroll, P. J.; Klein, M. L.; DeGrado, W. F. De Novo Design of Biomimetic Antimicrobial Polymers. *Proc. Natl. Acad. Sci. U.S.A.* **2002**, *99*, 5110−5114.

(23) Ergene, C.; Palermo, E. F. Self-Immolative Polymers with Potent and Selective Antibacterial Activity by Hydrophilic Side Chain Grafting. *J. Mater. Chem. B* **2018**, *6*, 7217−7229.

(24) Ergene, C.; Palermo, E. F. Cationic Poly(Benzyl Ether)S as Self-Immolative Antimicrobial Polymers. *Biomacromolecules* **2017**, *18*, 3400−3409.

(25) Lam, S. J.; O'Brien-Simpson, N. M.; Pantarat, N.; Sulistio, A.; Wong, E. H. H.; Chen, Y.-Y.; Lenzo, J. C.; Holden, J. A.; Blencowe, A.; Reynolds, E. C.; Qiao, G. G. Combating Multidrug-Resistant Gram-Negative Bacteria with Structurally Nanoengineered Antimicrobial Peptide Polymers. *Nat. Microbiol.* **2016**, *1*, 16162.

(26) Shirbin, S. J.; Lam, S. J.; Chan, N. J.-A.; Ozmen, M. M.; Fu, Q.; O'Brien-Simpson, N.; Reynolds, E. C.; Qiao, G. G. Polypeptide-Based Macroporous Cryogels with Inherent Antimicrobial Properties: The Importance of a Macroporous Structure. *ACS Macro Lett.* **2016**, *5*, 552−557.
(27) Yang, X.; Hu, K.; Hu, G.; Shi, D.; Jiang, Y.; Hui, L.; Zhu, R.; Xie, Y.; Yang, L. Long Hydrophilic-and-Cationic Polymers: A Different Pathway toward Preferential Activity against Bacterial over Mammalian Membranes. *Biomacromolecules* **2014**, *15*, 3267−3277.
(28) Punia, A.; He, E.; Lee, K.; Banerjee, P.; Yang, N.-L. Cationic Amphiphilic Non-Hemolytic Polyacrylates with Superior Antibacterial Activity. *Chem. Commun.* **2014**, *50*, 7071−7074.
(29) Michl, T. D.; Locock, K. E. S.; Stevens, N. E.; Hayball, J. D.; Vasilev, K.; Postma, A.; Qu, Y.; Traven, A.; Haeussler, M.; Meagher, L.; Griesser, H. J. Raft-Derived Antimicrobial Polymethacrylates: Elucidating the Impact of End-Groups on Activity and Cytotoxicity. *Polym. Chem.* **2014**, *5*, 5813−5822.
(30) Kuroda, K.; Caputo, G. A.; DeGrado, W. F. The Role of Hydrophobicity in the Antimicrobial and Hemolytic Activities of Polymethacrylate Derivatives. *Chem.—Eur. J.* **2009**, *15*, 1123−1133.
(31) Palermo, E. F.; Kuroda, K. Chemical Structure of Cationic Groups in Amphiphilic Polymethacrylates Modulates the Antimicrobial and Hemolytic Activities. *Biomacromolecules* **2009**, *10*, 1416−1428.
(32) Judzewitsch, P. R.; Nguyen, T.-K.; Shanmugam, S.; Wong, E. H. H.; Boyer, C. Towards Sequence-Controlled Antimicrobial Polymers: Effect of Polymer Block Order on Antimicrobial Activity. *Angew. Chem., Int. Ed.* **2018**, *57*, 4559−4564.
(33) Judzewitsch, P. R.; Zhao, L.; Wong, E. H. H.; Boyer, C. High-Throughput Synthesis of Antimicrobial Copolymers and Rapid Evaluation of Their Bioactivity. *Macromolecules* **2019**, *52*, 3975−3986.
(34) Hovakeemian, S. G.; Liu, R.; Gellman, S. H.; Heerklotz, H. Correlating Antimicrobial Activity and Model Membrane Leakage Induced by Nylon-3 Polymers and Detergents. *Soft Matter* **2015**, *11*, 6840−6851.
(35) Choi, H.; Chakraborty, S.; Liu, R.; Gellman, S. H.; Weisshaar, J. C. Single-Cell, Time-Resolved Antimicrobial Effects of a Highly Cationic, Random Nylon-3 Copolymer on Live Escherichia Coli. *ACS Chem. Biol.* **2016**, *11*, 113−120.
(36) Lienkamp, K.; Madkour, A. E.; Musante, A.; Nelson, C. F.; Nüsslein, K.; Tew, G. N. Antimicrobial Polymers Prepared by Romp with Unprecedented Selectivity: A Molecular Construction Kit Approach. *J. Am. Chem. Soc.* **2008**, *130*, 9836−9843.
(37) Ilker, M. F.; Nüsslein, K.; Tew, G. N.; Coughlin, E. B. Tuning the Hemolytic and Antibacterial Activities of Amphiphilic Polynorbornene Derivatives. *J. Am. Chem. Soc.* **2004**, *126*, 15870−15875.
(38) Ishitsuka, Y.; Arnt, L.; Majewski, J.; Frey, S.; Ratajczek, M.; Kjaer, K.; Tew, G. N.; Lee, K. Y. C. Amphiphilic Poly(Phenyleneethynylene)S Can Mimic Antimicrobial Peptide Membrane Disordering Effect by Membrane Insertion. *J. Am. Chem. Soc.* **2006**, *128*, 13123−13129.
(39) Uppu, D. S. S. M.; Samaddar, S.; Hoque, J.; Konai, M. M.; Krishnamoorthy, P.; Shome, B. R.; Haldar, J. Side Chain Degradable Cationic−Amphiphilic Polymers with Tunable Hydrophobicity Show in Vivo Activity. *Biomacromolecules* **2016**, *17*, 3094−3102.
(40) Stratton, T. R.; Howarter, J. A.; Allison, B. C.; Applegate, B. M.; Youngblood, J. P. Structure−Activity Relationships of Antibacterial and Biocompatible Copolymers. *Biomacromolecules* **2010**, *11*, 1286−1290.
(41) Tang, H.; Doerksen, R. J.; Tew, G. N. Synthesis of Urea Oligomers and Their Antibacterial Activity. *Chem. Commun.* **2005**, *12*, 1537−1539.
(42) Wang, C.; Zolotarskaya, O. Y.; Nair, S. S.; Ehrhardt, C. J.; Ohman, D. E.; Wynne, K. J.; Yadavalli, V. K. Real-Time Observation of Antimicrobial Polycation Effects on Escherichia Coli: Adapting the Carpet Model for Membrane Disruption to Quaternary Copolyoxetanes. *Langmuir* **2016**, *32*, 2975−2984.
(43) Palermo, E. F.; Vemparala, S.; Kuroda, K. Cationic Spacer Arm Design Strategy for Control of Antimicrobial Activity and Conformation of Amphiphilic Methacrylate Random Copolymers. *Biomacromolecules* **2012**, *13*, 1632−1641.
(44) Engler, A. C.; Tan, J. P. K.; Ong, Z. Y.; Coady, D. J.; Ng, V. W. L.; Yang, Y. Y.; Hedrick, J. L. Antimicrobial Polycarbonates: Investigating the Impact of Balancing Charge and Hydrophobicity Using a Same-Centered Polymer Approach. *Biomacromolecules* **2013**, *14*, 4331−4339.
(45) Palermo, E. F.; Kuroda, K. Structural Determinants of Antimicrobial Activity in Polymers Which Mimic Host Defense Peptides. *Appl. Microbiol. Biotechnol.* **2010**, *87*, 1605−1615.
(46) Palermo, E. F.; Lienkamp, K.; Gillies, E. R.; Ragogna, P. J. Antibacterial Activity of Polymers: Discussions on the Nature of Amphiphilic Balance. *Angew. Chem., Int. Ed.* **2019**, *131*, 3728−3731.
(47) Palermo, E. F.; Sovadinova, I.; Kuroda, K. Structural Determinants of Antimicrobial Activity and Biocompatibility in Membrane-Disrupting Methacrylamide Random Copolymers. *Biomacromolecules* **2009**, *10*, 3098−3107.
(48) Tew, G. N.; Scott, R. W.; Klein, M. L.; DeGrado, W. F. De Novo Design of Antimicrobial Polymers, Foldamers, and Small Molecules: From Discovery to Practical Applications. *Acc. Chem. Res.* **2010**, *43*, 30−39.
(49) Liu, R.; Chen, X.; Chakraborty, S.; Lemke, J. J.; Hayouka, Z.; Chow, C.; Welch, R. A.; Weisblum, B.; Masters, K. S.; Gellman, S. H. Tuning the Biological Activity Profile of Antibacterial Polymers Via Subunit Substitution Pattern. *J. Am. Chem. Soc.* **2014**, *136*, 4410−4418.
(50) Chakraborty, S.; Liu, R.; Hayouka, Z.; Chen, X.; Ehrhardt, J.; Lu, Q.; Burke, E.; Yang, Y.; Weisblum, B.; Wong, G. C. L.; Masters, K. S.; Gellman, S. H. Ternary Nylon-3 Copolymers as Host-Defense Peptide Mimics: Beyond Hydrophobic and Cationic Subunits. *J. Am. Chem. Soc.* **2014**, *136*, 14530−14535.
(51) Palermo, E. F.; Lee, D.-K.; Ramamoorthy, A.; Kuroda, K. Role of Cationic Group Structure in Membrane Binding and Disruption by Amphiphilic Copolymers. *J. Phys. Chem. B* **2011**, *115*, 366−375.
(52) Yang, Y.; Cai, Z.; Huang, Z.; Tang, X.; Zhang, X. Antimicrobial Cationic Polymers: From Structural Design to Functional Control. *Polym. J.* **2018**, *50*, 33−44.
(53) Ghose, A. K.; Viswanadhan, V. N.; Wendoloski, J. J. Prediction of Hydrophobic (Lipophilic) Properties of Small Organic Molecules Using Fragmental Methods: An Analysis of Alogp and Clogp Methods. *J. Phys. Chem. A* **1998**, *102*, 3762−3772.
(54) Sangster, J. *Octanol-Water Partition Coefficients: Fundamentals and Physical Chemistry*; John Wiley & Sons, 1997; Vol. *1*.
(55) Moad, G.; Rizzardo, E.; Thang, S. H. Living Radical Polymerization by the Raft Process. *Aust. J. Chem.* **2005**, *58*, 379−410.
(56) Chiefari, J.; Chong, Y. K.; Ercole, F.; Krstina, J.; Jeffery, J.; Le, T. P. T.; Mayadunne, R. T. A.; Meijs, G. F.; Moad, C. L.; Moad, G.; Rizzardo, E.; Thang, S. H. Living Free-Radical Polymerization by Reversible Addition−Fragmentation Chain Transfer: The Raft Process. *Macromolecules* **1998**, *31*, 5559−5562.
(57) Namivandi-Zangeneh, R.; Sadrearhami, Z.; Dutta, D.; Willcox, M.; Wong, E. H. H.; Boyer, C. Synergy between Synthetic Antimicrobial Polymer and Antibiotics: A Promising Platform to Combat Multidrug-Resistant Bacteria. *ACS Infect. Dis.* **2019**, *5*, 1357−1365.
(58) Nguyen, T.-K.; Lam, S. J.; Ho, K. K. K.; Kumar, N.; Qiao, G. G.; Egan, S.; Boyer, C.; Wong, E. H. H. Rational Design of Single-Chain Polymeric Nanoparticles That Kill Planktonic and Biofilm Bacteria. *ACS Infect. Dis.* **2017**, *3*, 237−248.
(59) Judzewitsch, P. R.; Nguyen, T.-K.; Shanmugam, S.; Wong, E. H. H.; Boyer, C. Towards Sequence-Controlled Antimicrobial Polymers: Effect of Polymer Block Order on Antimicrobial Activity. *Angew. Chem., Int. Ed.* **2018**, *57*, 4559−4564.
(60) Dai, Q.; Yan, Y.; Guo, J.; Björnmalm, M.; Cui, J.; Sun, H.; Caruso, F. Targeting Ability of Affibody-Functionalized Particles Is Enhanced by Albumin but Inhibited by Serum Coronas. *ACS Macro Lett.* **2015**, *4*, 1259−1263.
(61) Mowery, B. P.; Lindner, A. H.; Weisblum, B.; Stahl, S. S.; Gellman, S. H. Structure−Activity Relationships among Random

https://dx.doi.org/10.1021/acs.biomac.0c01320
Biomacromolecules XXXX, XXX, XXX−XXX

Nylon-3 Copolymers That Mimic Antibacterial Host-Defense Peptides. *J. Am. Chem. Soc.* **2009**, *131*, 9735−9745.
(62) Lambert, P. A. Cellular Impermeability and Uptake of Biocides and Antibiotics in Gram-Positive Bacteria and Mycobacteria. *J. Appl. Microbiol.* **2002**, *92*, 46s−54s.
(63) Shockman, G. D.; Barren, J. F. Structure, Function, and Assembly of Cell Walls of Gram-Positive Bacteria. *Annu. Rev. Microbiol.* **1983**, *37*, 501−527.
(64) Lienkamp, K.; Kumar, K.-N.; Som, A.; Nüsslein, K.; Tew, G. N. "Doubly Selective" Antimicrobial Polymers: How Do They Differentiate between Bacteria? *Chem.—Eur. J.* **2009**, *15*, 11710−11714.
(65) Oliver, S.; Wagh, H.; Liang, Y.; Yang, S.; Boyer, C. Enhancing the Antimicrobial and Antibiofilm Effectiveness of Silver Nanoparticles Prepared by Green Synthesis. *J. Mater. Chem. B* **2018**, *6*, 4124−4138.
(66) Zgurskaya, H. I.; López, C. A.; Gnanakaran, S. Permeability Barrier of Gram-Negative Cell Envelopes and Approaches to Bypass It. *ACS Infect. Dis.* **2015**, *1*, 512−522.
(67) Caroff, M.; Karibian, D. Structure of Bacterial Lipopolysaccharides. *Carbohydr. Res.* **2003**, *338*, 2431−2447.
(68) Qiao, J.; Liu, Z.; Purro, M.; Xiong, M. P. Antibacterial and Potentiation Properties of Charge-Optimized Polyrotaxanes for Combating Opportunistic Bacteria. *J. Mater. Chem. B* **2018**, *6*, 5353−5361.
(69) Magenau, A. J. D.; Richards, J. A.; Pasquinelli, M. A.; Savin, D. A.; Mathers, R. T. Systematic Insights from Medicinal Chemistry to Discern the Nature of Polymer Hydrophobicity. *Macromolecules* **2015**, *48*, 7230−7236.
(70) Petrauskas, A. A.; Kolovanov, E. A. Acd/Log P Method Description. *Perspect. Drug Discov. Des.* **2000**, *19*, 99−116.
(71) Dharmaratne, N. U.; Jouaneh, T. M. M.; Kiesewetter, M. K.; Mathers, R. T. Quantitative Measurements of Polymer Hydrophobicity Based on Functional Group Identity and Oligomer Length. *Macromolecules* **2018**, *51*, 8461−8468.
(72) Hu, K.; Schmidt, N. W.; Zhu, R.; Jiang, Y.; Lai, G. H.; Wei, G.; Palermo, E. F.; Kuroda, K.; Wong, G. C. L.; Yang, L. A Critical Evaluation of Random Copolymer Mimesis of Homogeneous Antimicrobial Peptides. *Macromolecules* **2013**, *46*, 1908−1915.
(73) Schmidt, N. W.; Lis, M.; Zhao, K.; Lai, G. H.; Alexandrova, A. N.; Tew, G. N.; Wong, G. C. L. Molecular Basis for Nanoscopic Membrane Curvature Generation from Quantum Mechanical Models and Synthetic Transporter Sequences. *J. Am. Chem. Soc.* **2012**, *134*, 19207−19216.
(74) Yang, L.; Gordon, V. D.; Mishra, A.; Som, A.; Purdy, K. R.; Davis, M. A.; Tew, G. N.; Wong, G. C. L. Synthetic Antimicrobial Oligomers Induce a Composition-Dependent Topological Transition in Membranes. *J. Am. Chem. Soc.* **2007**, *129*, 12141−12147.
(75) Yang, L.; Gordon, V. D.; Trinkle, D. R.; Schmidt, N. W.; Davis, M. A.; DeVries, C.; Som, A.; Cronan, J. E.; Tew, G. N.; Wong, G. C. L. Mechanism of a Prototypical Synthetic Membrane-Active Antimicrobial: Efficient Hole-Punching Via Interaction with Negative Intrinsic Curvature Lipids. *Proc. Natl. Acad. Sci. U.S.A.* **2008**, *105*, 20595−20600.
(76) Sgolastra, F.; deRonde, B. M.; Sarapas, J. M.; Som, A.; Tew, G. N. Designing Mimics of Membrane Active Proteins. *Acc. Chem. Res.* **2013**, *46*, 2977−2987.
(77) Kuroda, K.; DeGrado, W. F. Amphiphilic Polymethacrylate Derivatives as Antimicrobial Agents. *J. Am. Chem. Soc.* **2005**, *127*, 4128−4129.
(78) Sovadinova, I.; Palermo, E. F.; Huang, R.; Thoma, L. M.; Kuroda, K. Mechanism of Polymer-Induced Hemolysis: Nanosized Pore Formation and Osmotic Lysis. *Biomacromolecules* **2011**, *12*, 260−268.
(79) Yeaman, M. R.; Yount, N. Y. Mechanisms of Antimicrobial Peptide Action and Resistance. *Pharmacol. Rev.* **2003**, *55*, 27−55.
(80) Paterson, D. J.; Tassieri, M.; Reboud, J.; Wilson, R.; Cooper, J. M. Lipid Topology and Electrostatic Interactions Underpin Lytic Activity of Linear Cationic Antimicrobial Peptides in Membranes. *Proc. Natl. Acad. Sci. U.S.A.* **2017**, *114*, E8324−E8332.
(81) Ikonen, E. Cellular Cholesterol Trafficking and Compartmentalization. *Nat. Rev. Mol. Cell Biol.* **2008**, *9*, 125−138.
(82) O'Connor, C. M.; Adams, J. U. *Essentials of Cell Biology*; NPG Education: Cambridge MA, 2010.
(83) Yeagle, P. L. Cholesterol and the Cell Membrane. *Biochim. Biophys. Acta Rev. Biomembr.* **1985**, *822*, 267−287.
(84) Raffy, S.; Teissié, J. Control of Lipid Membrane Stability by Cholesterol Content. *Biophys. J.* **1999**, *76*, 2072−2080.
(85) Matsuzaki, K.; Sugishita, K.; Fujii, N.; Miyajima, K. Molecular Basis for Membrane Selectivity of an Antimicrobial Peptide, Magainin 2. *Biochemistry* **1995**, *34*, 3423−3429.
(86) Matsuzaki, K. Why and How Are Peptide−Lipid Interactions Utilized for Self-Defense? Magainins and Tachyplesins as Archetypes. *Biochim. Biophys. Acta* **1999**, *1462*, 1−10.

https://dx.doi.org/10.1021/acs.biomac.0c01320
Biomacromolecules XXXX, XXX, XXX−XXX